Emerging Microbes & Infections
2025, VOL. 14, 2477645 (14 pages)
https://doi.org/10.1080/22221751.2025.2477645

Eukaryotic RNA binding protein hnRNPH1 suppresses influenza A virus replication through interaction with virus NS1 protein

Jinyu Wang[a], Yang Zhang[a,b], Lishan Sun[a], Zihan Wang[a], Cui Hao[c] and Wei Wang [a,b]

[a]Key Laboratory of Marine Drugs, Ministry of Education, School of Medicine and Pharmacy, Ocean University of China, Qingdao, People's Republic of China; [b]Laboratory for Marine Drugs and Bioproducts, Qingdao Marine Science and Technology Center, Qingdao, People's Republic of China; [c]Medical Research Center, The affiliated Hospital of Qingdao University, Qingdao, People's Republic of China

ABSTRACT

The NS1 protein of influenza A virus (IAV) is a multi-functional protein which can antagonize host immune system and facilitate viral replication by interacting with host factors. However, the novel partners in host cells interacting with NS1 need to be fully elucidated. In the current study, we identified hnRNPH1 as a novel binding partner of NS1 to regulate IAV replication. Notably, overexpression of hnRNPH1 decreased IAV multiplication, while knockdown of hnRNPH1 enhanced IAV replication. hnRNPH1 can interact with NS1 to change the intracellular localization and splicing function of NS1, and impact IAV replication through interacting with p53 to regulate cell apoptosis. In addition, the RBD domain of NS1 and the RRM and NLS regions of hnRNPH1 may be the major sites for their interaction. In summary, our studies identified hnRNPH1 as a novel NS1-binding protein and elucidated its regulatory roles in IAV replication, which will provide new insights into the roles of NS1 binding proteins, and give a reference for anti-IAV therapy based on NS1-host interaction.

ARTICLE HISTORY Received 15 November 2024; Revised 30 January 2025; Accepted 5 March 2025

KEYWORDS Influenza A virus; NS1 protein; hnRNPH1; viral replication; interaction mode

Introduction

Influenza A Virus (IAV) is a negative-sense single-stranded RNA virus with envelope that belongs to *Orthomyxoviridae*, and can be divided into several subtypes, such as H1N1 and H3N2 [1]. IAV is a most formidable pathogen, which has been the cause of at least three pandemics in the last century [2]. The genome of IAV comprises eight segments, encoding a total of 19 proteins [3,4]. The main structure proteins of IAV includes nucleocapsid protein (NP), RNA polymerase complex (PA, PB1, PB2) [5,6], matrix protein (M1, M2) [7–9], haemagglutinin (HA), and neuraminidase (NA) [10]. Besides, two main non-structural proteins are produced through NS gene splicing as NS1 and NS2 [11]. The non-structural protein 1 (NS1) is the key virulence factor of IAV in antagonizing interferon system, inhibiting host mRNA processing, promoting viral protein synthesis, and regulating cell apoptosis [12–15]. Thus, NS1 is considered to be an important co-factor in viral pathogenesis and may be a novel target for anti-IAV therapy.

NS1 is approximately 26 kD and contains 215–237 amino acids, with slight differences among different subtype strains [12]. It contains two important functional regions, RNA binding domain (RBD) and effector domain (ED), connected by a linking region (LR) of 7–12 amino acids [12]. NS1 mainly appears as a homodimer in cells which comprises two RBD and an entangled dimeric ED. Our previous studies discovered that NS1 can bind to the mRNAs of viral late genes so as to promote the nuclear export of virus mRNA via cellular NXF1/P15 pathway rather than CRM1 dependent pathway [16]. Besides that, NS1 can also interact with various cellular factors such as CPSF and PABII, thereby inhibiting host mRNA splicing and enhancing virus replication [15]. Therefore, revealing the interaction between NS1 and host proteins is of great significance for elucidating the pathogenic mechanism of IAV.

The hnRNPs represent a family of about twenty single-stranded RNA-binding proteins associated with multiple cellular functions, including mRNA splicing and translational regulation [17]. Besides that, hnRNPs were also found to assist in regulating viral replication in different ways. The hnRNPH1 belongs to the hnRNP F/H subfamily, which is

CONTACT Wei Wang wwwakin@ouc.edu.cn Key Laboratory of Marine Drugs, Ministry of Education, School of Medicine and Pharmacy, Ocean University of China, Qingdao 266003, People's Republic of China Laboratory for Marine Drugs and Bioproducts, Qingdao Marine Science and Technology Center, Qingdao 266237, People's Republic of China

Supplemental data for this article can be accessed online at https://doi.org/10.1080/22221751.2025.2477645.

primarily responsible for processes such as mRNA transcription and splicing [18]. hnRNPH1 contains a total of three quasi-RRMs (qRRM) [19] as well as two glycine-rich structural domains (GRD). The central GRD contains a segment of NLS, which is essential for hnRNPH1's interaction with the nuclear entry receptor (transportin 1, Trn1) to enable the nucleoplasmic shuttling of hnRNPH1 [20]. Notably, hnRNPH1 has the ability to enhance viral replication by binding to the V protein of Newcastle disease virus, as well as promoting viral gene replication through interactions with viral RNA and proteins [21].

In the present study, hnRNPH1 was identified as a novel NS1 binding protein by using pull-down assay combined with co-immunoprecipitation. This study aimed to characterize the interaction between hnRNPH1 and NS1, and investigate the roles of hnRNPH1 in IAV replication. Our studies indicated that hnRNPH1 could interact with NS1 and influence the replication of IAV. The interaction between hnRNPH1 and NS1 can influence the splicing function of NS1, and impacting IAV replication through apoptosis regulation. Moreover, the RBD domain of NS1 and the RRM regions of hnRNPH1 may be the major sites for their interaction. In summary, this is the first report that provides evidence that hnRNPH1 exerts the regulatory roles in IAV replication through interaction with NS1.

Materials and methods

Reagents, cells, and viruses

Protein A/G and Anti-Flag/Myc magnetic beads were purchased from MedChemexpress (NJ, USA). The following antibodies were used in this study: anti-Flag (Yeason, Shanghai, China), anti-Myc (Abbkine, Wuhan, China), anti-NS1 (GeneTex, CA, USA), anti-HA (Sino Biological, Beijing, China), anti-NP (Sino Biological, Beijing, China), anti-β-actin (Abways, Shanghai, China), anti-Tubulin (Abways, Shanghai, China). A549 cells were cultured in Ham's F-12 K medium supplemented with 10% fetal bovine serum (FBS), penicillin (100 U/mL), and streptomycin (100 μg/mL). MDCK cells were grown in Eagle's minimum essential medium (EMEM) supplemented with 10% FBS, 100 U/mL of penicillin, and 100 μg/mL of streptomycin. 293 T cells were cultured in Dulbecco's modified Eagle's medium (DMEM) supplemented with 10% FBS, 100 U/mL of penicillin, and 100 μg/mL of streptomycin. Influenza H1N1 virus (A/Puerto Rico/8/34 [H1N1]; PR/8) and (A/WSN/1933 [H1N1]; WSN) were propagated in 9-day-old embryonated eggs for 3 days at 36.5°C. Influenza H3N2 virus (A/Aichi/2/68) was propagated in MDCK cells at 37°C for 3 days.

Construction of NS1 and hnRNPH1 plasmids

The sequences of PR8 NS1 and hnnRNP H1 were obtained from the National Center for Biotechnology Information (NCBI), and primers were synthesized by Sangon (Shanghai, China). The VC155-NS1 overexpression plasmids were constructed with VC-155-HA vector, and the VN173-hnRNPH1, VN173-hnRNPH1-R1R2, VN173-hnRNPH1-ΔR3GY and VN173-hnRNPH1-ΔGY plasmids were constructed with VN-173-Flag vector. The cell RNA was first reverse transcriped using Evo M-MLV Plus 1st Strand cDNA Synthesis Kit (Accurate Biology, Hunan, China), and then PCR was performed using ApexHF HS DNA polymerase CL (Accurate Biology, Hunan, China). The primers for construction are shown in supplementary Table S2. The DNA was purified using a gel extraction kit (Yeasen, Shanghai, China). Then the vector and purified DNA were digested with certain endonuclease and ligated using T4 ligase (Takara, Shiga, Japan) for 16°C 45 min, and finally the plasmids were transformed into DH5α or Top 10.

Pull-down assay

PR8 virus (MOI = 3.0) infected A549 cells were lysed for 15–20 min on ice by using 600 μL of IP lysis buffer containing 1 × cocktail protease inhibitor. After that, the supernatant of cell lysate was collected into 1.5 mL centrifuge tube and then incubated with anti-NS1 antibody at 4°C overnight. Then the protein A/G magnetic beads were added and incubated with cell lysate at 4°C overnight. Then the immunoprecipitates were separated in a denaturing gel and coomassie blue stained. Bands detected only in immunoprecipitates were excised and digested with trypsin to purify peptides before analysis with a tandem mass spectrometer (LC-MS/MS; Q-Star Elite, Applied Biosystems). The peptide masses obtained by LC-MS/MS analysis were then processed against human protein sequences in the National Center for Biotechnology Information (NCBI) RefSeq database using the Mascot algorithm (Matrix Science).

Western blot assay

The cell lysates were separated by SDS-PAGE and transferred to nitrocellulose membrane. After being blocked in Tris-buffered saline (TBS) containing 0.1% Tween 20 (v/v) and 5% BSA (w/v) at 37°C for 2 h, the membranes were rinsed and incubated at 4°C overnight with primary antibodies. The membranes were washed and incubated with AP-labelled secondary antibody (1:5000 dilutions) at 37°C for 2 h. The protein bands were then visualized by incubating with the developing solution (p-nitro blue

tetrazolium chloride (NBT) and 5-bromo-4-chloro-3-indolyl phosphate toluidine (BCIP)). The relative densities of proteins were all determined by using ImageJ (NIH) v.1.33 u (USA).

Quantitative RT–PCR assay

Firstly, the total RNA was extracted from IAV infected cells by using the RNA extraction kit (Aidlab, Beijing, China), and then the gDNA was removed and RNA was reverse transcriped according to the manufacturer's instructions. The reaction was carried out at 37°C for 15 min, 85°C for 5 s, and 4°C for 5 min. After that, the qPCR reaction solution was prepared according to the instructions. And fluorescence quantification was performed according to the recommended procedure in the instruction manual.

Co-immunoprecipitation assay

293 T cells were first transfected or co-transfected with plasmids encoding NS1 and hnRNPH1 proteins. After 24 h, 293 T cells were lysed on ice for 20 min, and then the supernatant was incubated with Anti-Flag or Anti-Myc magnetic beads overnight at 4°C. After that, the incubated beads were washed three times and then subjected to 10% SDS-PAGE. Binding of hnRNPH1 or NS1 to the beads was detected by western blotting using the anti-hnRNPH1 or NS1 antibodies, respectively. The relative densities of proteins were all determined by using ImageJ (NIH) v.1.33 u (USA).

Interferon promoter-based luciferase reporter assay

293 T cells were transfected with 0.2 μg of the reporter plasmid p125Luc, 0.2 μg of renilla-luc plasmid, and 0.6 μg of pcDNA3.1-NS1 (PR8) using Polyfect transfection reagent (Invitrogen Lipofectamine 2000) with or without hnRNPH1-flag or hnRNPH1 siRNA transfection. At 16 h post-transfection, the cells were stimulated with 50 μg of poly[IC] (Sigma-Aldrich)/ml for 16 h. Then the cells were lysed with 1 × passive lysis buffer (Promega), and 20 μl of the lysate was used to measure the luciferase activities using the Dual luciferase reporter assay system (Promega) according to the manufacturer's protocol.

Plaque assay

Confluent MDCK cell monolayers in 12-well plates were incubated with cell supernatants harvested from other experiments at 37°C for 1 h. After removal of the inoculum, cells were washed with PBS and overlaid with maintenance DMEM medium containing 1.7% agarose, 0.02% DEAE-dextran, 1 mM L-glutamine, 0.1 mM non-essential amino acids, 100 U/mL penicillin, 100 μg/mL streptomycin and 1 μg/mL TPCK-treated trypsin. After incubation for 3 days at 37°C in a humidified atmosphere of 5% CO_2, cells were fixed with 4% paraformaldehyde, followed by staining with 1% crystal violet in 20% ethanol for plaque counting.

Indirect immunofluorescence assay

MDCK or A549 cells were first infected with PR8 virus (MOI = 1.0) for different time duration (4, 6, 8 h), then the cells were washed with PBS and fixed with 4% paraformaldehyde for 10 min. After that, the cells were incubated with 2% BSA/PBS for 1 h at 37°C before permeabilized using 0.5% (v/v) Triton X-100 in PBS for 10 min. Cells were then washed and incubated with anti-NS1 or hnRNPH1 antibodies overnight at 4°C. After washing, the cells were incubated with FITC/Dylight 649-conjugated secondary antibody (Boster, Wuhan, China) for 1 h at 37°C. Nuclear DNA was labelled with DAPI (Beyotime, Shanghai, China) for 10 min. Finally, the cells were washed and observed using confocal laser scanning microscope (Leica, Germany).

Statistical analysis

All data are representative of at least three independent experiments. Statistical significance was calculated by GraphPad Prism 9.0 (San Diego, CA, USA) using one-way ANOVA analysis followed by post hoc Tukey's tests if F achieved statistical significance ($p < 0.05$) and there was no significant variance in homogeneity. Statistical significance was considered to be $p < 0.05$.

Results

Identification and validation of novel NS1-interacting proteins

In this study, we initially identified NS1-interacting proteins in A549 cells *via* pull-down assay combined with mass spectrometry (Figure 1(A and B) and Table S1). Then, the potential target proteins ALDH1A1, eEF1A1 and hnRNPH1 were validated in A549 cells by western blot (Figure S1A), and all three proteins bound well to NS1. As A549 is a type of tumour cell, we quantified the abundance of these three candidate proteins in different cells involved (Figure 1(C)). The eEF1A1 and hnRNPH1 proteins expressed in these four cells, and only hnRNPH1 expressed homogeneously at a high level. ALDH1A1, a common cancer marker, was only highly expressed in A549 (Figure 1(C)). Thus, we mainly focus our studies on hnRNPH1 protein in the subsequent experiments. To

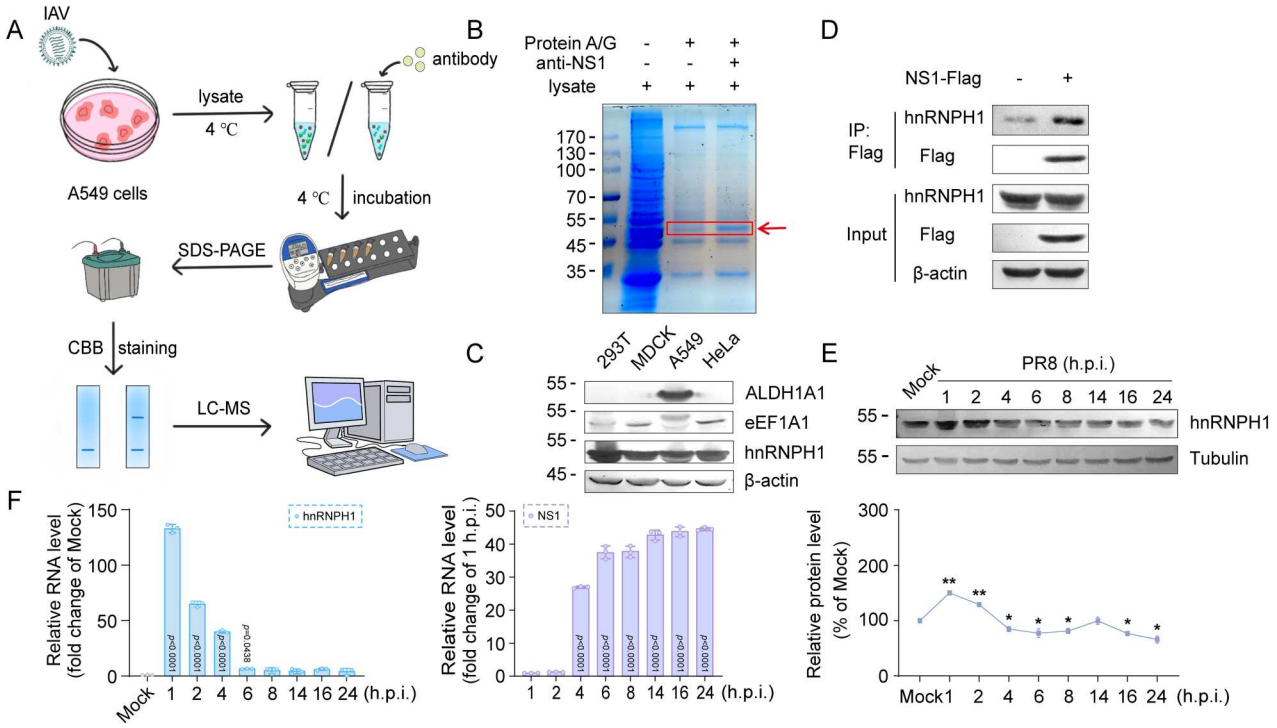

Figure 1. hnRNPH1 interacts with IAV NS1 protein. (A) The flowchart of pull-down assay. Lysates of PR8-infected A549 cells were collected and incubated with NS1 antibody at 4°C overnight, followed by incubation with protein A/G. SDS-PAGE was performed and the sample was analyzed using LC-MS. (B) Protein A/G were incubated with NS1 antibody, and then incubated with lysate of A549 cells infected with PR8 virus (MOI = 11). SDS-PAGE was performed. (C) The cellular abundance of hnRNPH1 was examined in A549, 293 T and MDCK, and HeLa was used as a tumour cell control. (D) NS1-Flag was first enriched in 293 T using anti-Flag beads and then incubated with MDCK lysate for co-IP. (E and F) hnRNPH1 levels in PR8 infected A549 cells (MOI = 0.1) at different moments were detected. hnRNPH1 protein levels were revealed by western blot. The expression level of hnRNPH1 was quantified using Image J as fold change after normalized to tubulin. Values are means ± S.D. ($n = 3$). *$p < 0.05$, **$p < 0.01$ vs. Mock (E). The RNA levels of hnRNPH1 were revealed by qPCR. The relative amounts of hnRNPH1 and NS1 mRNAs were determined using the comparative ($2^{-\Delta\Delta Ct}$) method. Values are means ± S.D. ($n = 3$). *P* values vs. Mock (left) and vs. 1 h.p.i. (right) are shown in the figure (F).

further validate the interaction between endogenous hnRNPH1 and NS1, pcDNA3.1-NS1-Flag was transfected into 293 T cells and the immunoprecipitated proteins were identified by western blot (Figure 1(D)). We found that hnRNPH1 can truly bind to NS1 in a specific manner, suggesting that hnRNPH1 is a potential interacting protein of NS1.

To preliminary elucidate the influence of IAV on hnRNPH1 expression, the expression levels of hnRNPH1 was tested in PR8 (A/Puerto Rico/8/1934(H1N1)) infected A549 cells at different time points by using western blot and qPCR (Figure 1(E and F)). The results indicated that PR8 infection initially induced a slight increase in the protein level of hnRNPH1 at 1 h.p.i., followed by a subsequent continuous decrease within 24 h (Figure 1(E)). The change of hnRNPH1 RNA levels was slightly different from that of protein levels (Figure 1(F)). It increased rapidly at 1 h.p.i. and then continued to decline until 6 h.p.i., but remained slightly higher than those of the non-infected group within 24 h (Figure 1(F)). In contrast, the RNA levels of NS1 increased quickly after 4 h.p.i. and remained high levels within 24 h. Taken together, we speculate that the increase of hnRNPH1 may be attributed to the cellular stress in response to IAV infection and the subsequent decrease may be related to the inhibition of host gene expression by NS1.

To further explore the effects of different MOIs of PR8 virus on hnRNPH1 expression, the western blot and qPCR were used to detect the protein and mRNA levels of hnRNPH1. The results showed that there were no significant difference in the protein and mRNA levels of hnRNPH1 after PR8 infection at different MOIs (MOI = 0.1, 1, 10) (Figure S1B and C). Besides, the overexpression and interference of hnRNPH1 had similar regulatory effects on viral replication in cells infected with different MOIs of PR8 (Figure S1D and E), suggesting that the interaction between hnRNPH1 and NS1 may be not affected by the amount of viral infection. In conclusion, we successfully identified hnRNPH1 as a new NS1-interacting protein, and hnRNPH1 responded to IAV infection at different times in terms of both protein and RNA levels.

Inhibition of viral proliferation by hnRNPH1 overexpression

To further verify the interaction between NS1 and hnRNPH1, pcDNA3.1-hnRNPH1-Flag and pcDNA3.1-NS1-Myc were co-transfected into 293 T

cells and then the co-immunoprecipitation (Co-IP) assay was performed. The results demonstrated that NS1-Myc could co-immunoprecipitate with hnRNPH1-Flag (Figure 2(A)), and hnRNPH1-Flag also co-immunoprecipitated efficiently with NS1-Myc (Figure 2(B)). The results of surface plasmon resonance (SPR) assay also showed that hnRNPH1 can bind specifically to NS1 with a KD value of about 10.37 μM (Figure S2A). Moreover, the combination of the two was dependent on RNA (Figure 2(C)). Next, we evaluated the influence of hnRNPH1 on IAV replication in A549 cells by using western blot and quantitative RT–PCR. hnRNPH1 overexpression resulted in a significant and dose-dependent decrease in the expression of HA and NS1 proteins, suggesting that hnRNPH1 possesses a negative regulation effect on virus protein expression (Figure S2B and Figure 2(D)). Similarly, the RNA levels of NS1 and NA proteins were both significantly decreased after hnRNPH1 overexpression (Figure 2(E)), demonstrating that hnRNPH1 also negatively regulated the RNA levels of IAV proteins.

To further evaluate the influence of hnRNPH1 on viral multiplication over multiple life cycles, we then detected the viral titers at different time points (12, 24, 36 h.p.i.) after hnRNPH1 overexpression by using plaque and HA titer assay. The overexpression of hnRNPH1 resulted in a significant reduction of viral titer in a dose-dependent manner (Figure 2(F) and S2C). In addition, to investigate whether hnRNPH1 has a broad-spectrum effect on influenza viruses, we also examined the effect of hnRNPH1 overexpression on the infection of H3N2 (A/Aichi/2/1968 (H3N2)) and WSN (A/WSN/1933 (H1N1)). The results showed that hnRNPH1 overexpression had inhibition effects on the proliferation of both H3N2 and WSN although the inhibition of WSN was weaker than that of H3N2 (Figure S2D and 2E), suggesting that hnRNPH1

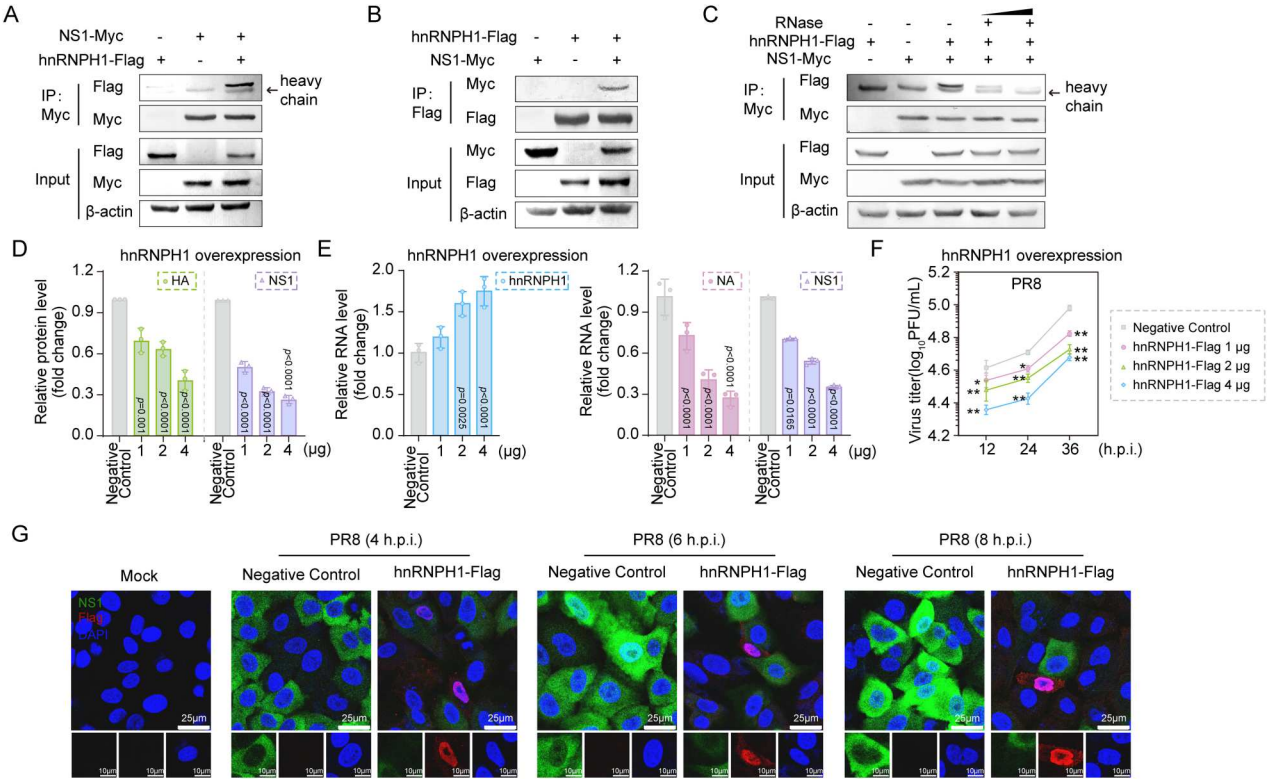

Figure 2. hnRNPH1 overexpression can inhibit IAV proliferation. (A and B) hnRNPH1-NS1 interaction was validated of by Co-IP. NS1 and hnRNPH1 were co-transfected into 293 T. hnRNPH1-Flag was fished using anti-Myc magnetic beads binding NS1-Myc (A). And NS1-Myc was fished using anti-Flag magnetic beads combined with hnRNPH1-Flag (B). (C) NS1-Myc and hnRNPH1-Flag were co-transfected into 293 T cells. All the cell lysates were treated without or with RNase (10 and 100 μg/mL) at 37°C for 15 min, and then the hnRNPH1-Flag was fished using anti-Myc magnetic beads binding NS1-Myc. (D and E) The effects on IAV proteins after overexpression of hnRNPH1 was investigated. A549 cells were transfected with hnRNPH1-Flag. At 36 h post-transfection, cells were infected with PR8 (MOI = 0.1). The protein level of hnRNPH1, IAV HA and NS1 was revealed by western blot. The expression level of HA and NS1 was quantified using Image J as fold change after normalized to β-actin. Values are means ± S.D. (n = 3). *P* values vs. Negative Control are shown in the figure (D). The RNA level of hnRNPH1, IAV NA and NS1 was detected by qPCR. The relative amounts of mRNAs were determined using the comparative ($2^{-\Delta\Delta Ct}$) method. Values are means ± S.D. (n = 3). *P* values vs. Negative Control are shown in the figure (E). (F) hnRNPH1 transfected A549 was infected with PR8 (MOI = 0.1) at 36 h post-transfection, and supernatants were collected for plaque assay. $*p < 0.05$, $**p < 0.01$ vs. Negative Control. (G) A549 cells were transfected with hnRNPH1-Flag. At 36 h post-transfection, cells were infected with PR8 (MOI = 10). At 4, 6, 8 h.p.i., cells were fixed with 4% PFA and the co-localization of NS1 with hnRNPH1 was detected by fluorescence microcopy. Scale bars represent 25 and 10 μm.

overexpression may be able to downregulate the multiplication of different IAV subtypes. Moreover, we also performed immunofluorescence assay to explore the influence of hnRNPH1 on NS1 expression and localization in A549 cells. As shown in Figure 2G, after overexpression of hnRNPH1, the fluorescence of NS1 significantly decreased as compared to that in the negative control group, suggesting that hnRNPH1 overexpression can suppress the expression of NS1 rather than change its localization. Taken together, all these results indicated that overexpression of hnRNPH1 may be able to inhibit the proliferation of IAV from RNA level.

Promotion of viral proliferation by hnRNPH1 interference

To further evaluate the effect of hnRNPH1 knockdown on IAV replication, two synthesized siRNAs were transfected into A549 cells. As shown in Figure 3A, sihnRNPH1-1 significantly reduced the expression of hnRNPH1, superior to the effects of sihnRNPH1-2 and the irrelevant negative control siRNA. Thus, the sihnRNPH1-1 was selected for the subsequent experiments. The effects of hnRNPH1 knockdown on IAV replication were then evaluated by performing western blot and qRT-PCR. The results showed that cells transfected with sihnRNPH1-1 (80, 120 nM) had a significantly higher level of NS1 and HA gene expression as compared to the negative control (Figure S3A and Figure 3(B)), suggesting that knockdown of hnRNPH1 can increase viral replication. Consistently, the results of qRT-PCR indicated that hnRNPH1 knockdown can also dose-dependently increase the RNA levels of both NS1 and NA proteins in A549 cells (Figure 3(C)).

Subsequently, we conducted growth curve analysis to further evaluate the influence of hnRNPH1 knockdown on viral multiplication over multiple life cycles by using plaque and HA titer assay. Notably, there was a significant increase in viral titers at various time points after interference of hnRNPH1 in a dose-dependent manner (Figure 3(D) and S3B). Moreover, we similarly examined the effect of hnRNPH1 interference on A549 cells infected with H3N2 and WSN virus, and the results indicated that hnRNPH1 knockdown indeed promoted the proliferation of different IAV subtypes (Figure S3C and 3D).

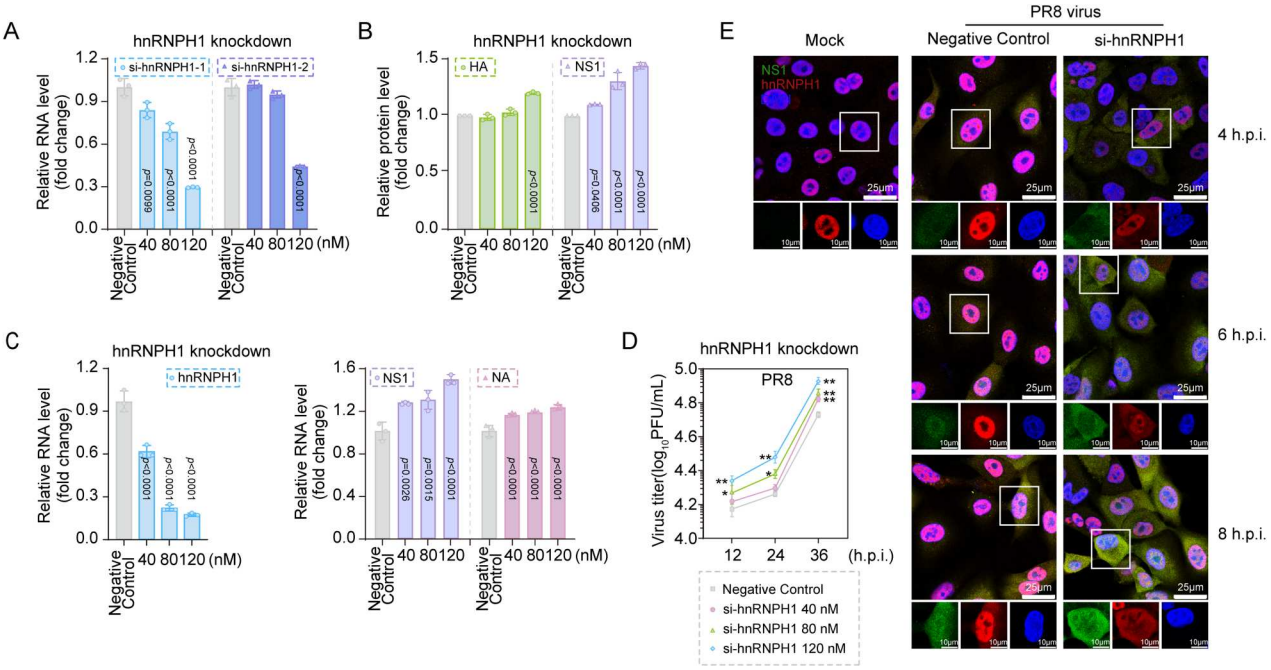

Figure 3. Interference of hnRNPH1 can promote IAV proliferation. (A) A549 cells were transfected with different siRNAs. The RNA level of hnRNPH1 was detected by qPCR. The relative amounts of mRNAs were normalized using the comparative ($2^{-\Delta\Delta Ct}$) method. Values are means ± S.D. ($n = 3$). *P* values vs. Negative Control are shown in the figure. (B and C) The effects on IAV proteins after interference of hnRNPH1 were investigated. A549 cells were transfected with si-hnRNPH1. At 36 h interference, cells were infected with PR8 (MOI = 0.1). The protein level of hnRNPH1, IAV HA and NS1 was revealed by western blot. The expression level of HA and NS1 was quantified using ImageJ as fold change after normalized to β-actin. Values are means ± S.D. ($n = 3$). *P* values vs. Negative Control are shown in the figure (B). The RNA level of hnRNPH1, IAV NA and NS1 was detected by qPCR. The relative amounts of mRNAs were determined using the comparative ($2^{-\Delta\Delta Ct}$) method. Values are means ± S.D. ($n = 3$). *P* values vs. Negative Control are shown in the figure (C). (D) siRNA interfered A549 was infected with PR8 (MOI = 0.1) at 36 h post-transfection, and supernatants were collected for plaque assay. Values are means ± S.D. (n = 3). $^*p < 0.05$, $^{**}p < 0.01$ vs. Negative Control. (E) A549 cells were interfered with si-hnRNPH1. At 36 h post-transfection, cells were infected with PR8 (MOI = 10). At 4, 6, 8 h.p.i., cells were fixed with 4% PFA and the co-localization of NS1 with hnRNPH1 was detected by fluorescence microcopy. Scale bars represent 25 and 10 μm.

Thus, by integrating the results of all experiments involving hnRNPH1 overexpression and interference, we identified hnRNPH1 as an antiviral factor to different IAV subtypes. To further investigate the influence of hnRNPH1 knockdown on the expression and localization of NS1, the immunofluorescence assay was employed in PR8 infected A549 cells after hnRNPH1 interference. The fluorescence of NS1 significantly increased after hnRNPH1 interference, particularly at 6–8 h.p.i. (Figure 3(E)), suggesting that hnRNPH1 interference may facilitate viral replication. Meanwhile, hnRNPH1 was observed to shift to the cytoplasm upon IAV infection, and gradually increased from 6 to 8 h.p.i., indicating a change in its cellular localization (Figure 3(E)).

Furthermore, despite an overall decrease in fluorescence intensity following hnRNPH1 interference, there was an increase of hnRNPH1 localization in cytoplasm and showed significant co-localization with NS1. This phenomenon may be due to the weakened hnRNPH1 restriction on virus replication, and virus utilizes alternative pathways to expedite its proliferation, while inducing the hnRNPH1 to react to viral proliferation by enhancing nucleoplasmic shuttling. This represents a bi-directional regulatory relationship between virus and its host. In summary, hnRNPH1 interference can enhance IAV infection from RNA level and promote the nucleocytoplasmic shuttling of virus proteins.

Endogenous and exogenous hnRNPH1 both co-localize with NS1

To further examine the interaction between hnRNPH1 and NS1, we constructed two BiFC plasmids, VC155-NS1 and VN173-hnRNPH1, to detect the colocalization of these two proteins in non-infected A549 cells. There was no green fluorescence in the VC155-NS1 or VN173-hnRNPH1 singly transfected cells but strong fluorescence could be observed in the positive control group (VC155 + VN173), suggesting that the BiFC system was successfully established (Figure 4(B)). However, specific green fluorescence could be observed in the nucleus of VC155-NS1 and VN173-hnRNPH1 co-transfected A549 cells (Figure 4(B)), suggesting that NS1 and hnRNPH1 can truly interact with each other mainly in cell nucleus.

Subsequent confocal observation of exogenously expressed hnRNPH1 and NS1 in A549 cells revealed notable co-localization primarily in the nucleus, but with slight co-localization in the cytoplasm (Figure 4(C)). To further evaluate the co-localization of endogenous hnRNPH1 and NS1 in IAV infected MDCK cells, and also to validate the nucleoplasmic shuttling of hnRNPH1 we found before, we performed immunofluorescence assay at different time points after virus infection (4, 6 and 8 h.p.i.). hnRNPH1 began to translocate to the cytoplasm at 4 h.p.i., and gradually accumulated in the cytoplasm over time, and reached the peak at 8 h.p.i. (Figure 4(D)). Strong co-localization of NS1 and hnRNPH1 was observed in both cytoplasm and nucleus (Table S4). To further explore whether hnRNPH1 can alter mRNA stability or nuclear export, we performed nucleoplasmic isolation experiments to detect the changes of mRNA contents in both the nucleus and cytoplasm (Figure 4(E)). The results showed that the nucleoplasmic ratio of NS1 and hnRNPH1 mRNAs continuously decreased from 4 to 8 h.p.i., suggesting that the nuclear export and expression of hnRNPH1 mRNA may enhance the export of virus mRNAs after 4 h infection.

In conclusion, these results suggest the possibility of simultaneous co-localization of NS1 and hnRNPH1 in the nucleus and cytoplasm of IAV-infected cells, and the nucleoplasmic transfer of hnRNPH1 may influence the export of viral proteins from the nucleus.

hnRNPH1 affects NS1 function by regulating apoptosis and NS1 splicing

To further investigate which process of viral infection is specifically affected by hnRNPH1, we decreased the levels of hnRNPH1 using siRNA in A549 cells before performing the immunofluorescence assay of viral proteins at different time points after virus infection. The results showed that hnRNPH1 knockdown did not affect the process of viral entry (Figure 5(A)), uncoating (Figure 5(B)), and vRNP nuclear import (Figure 5(C)). However, at 4 h.p.i., the knockdown of hnRNPH1 had already significantly enhanced the expression of virus NP protein, consistent to the previous results (Figure 5(C)).

Afterwards, we considered the possibility that hnRNPH1 regulation of viruses may be at a later stage of viral infection or other host functions. Following IAV infection, the NS1 protein can exert a notable antagonist effect on the host innate immune response. To investigate the influence of hnRNPH1 on the interferon antagonist function of NS1, we conducted an IFN-β reporter assay in the presence of hnRNPH1 overexpression or knockdown (Figure 5(D)). The overexpression of hnRNPH1 significantly restored the induction levels of the IFN-β reporter which was reduced by NS1 in a dose-dependent manner (Figure 5(E)), suggesting that the elevation of hnRNPH1 may impede NS1 function, leading to a notable inhibition of interferon antagonist effect. Conversely, interference with hnRNPH1 resulted in a dose-dependent decrease in the levels of IFN-β reporter, indicating that the interaction between hnRNPH1 and NS1 may regulate the function of NS1 related to interferon system, due to the inhibition of NS1 by

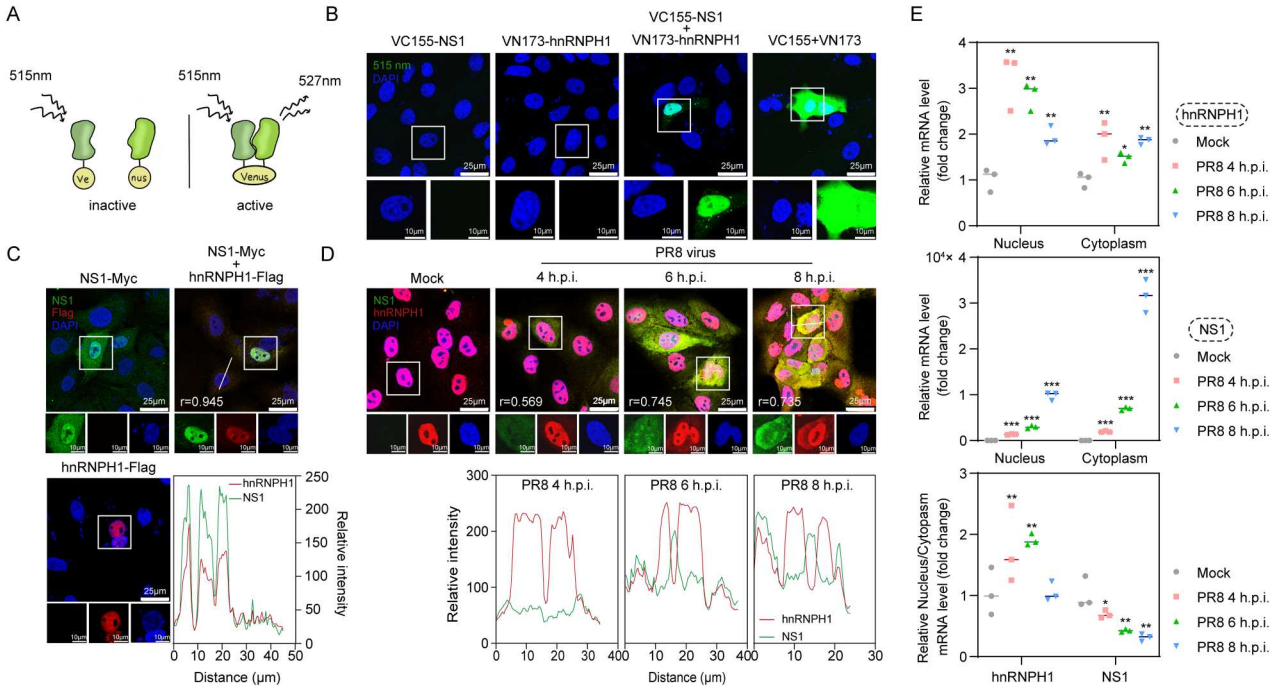

Figure 4. Endogenous and exogenous hnRNPH1 co-localize with NS1. (A) The excitation and emission wavelengths of BiFC fluorescent proteins. BiFC fluorescence is excited at 515 nm and detected at 527 nm. (B) A549 cells were transfected with VC155-NS1 and VN173-hnRNPH1. At 36 h post-transfection, cells were fixed and the co-localization of NS1 with hnRNPH1 was detected by fluorescence microcopy. Scale bars represent 25 and 10 μm. (C) A549 cells were transfected with NS1-Myc and hnRNPH1-Flag. Cells were fixed and the co-localization of NS1 with hnRNPH1 was detected by fluorescence microcopy after 36 h. Scale bars represent 25 and 10 μm. Co-localization was analyzed by Image J. The person's correlation coefficient is shown in the figure. (D) PR8 (MOI = 10) infected A549 cells were fixed at 4, 6, 8 h.p.i.. The co-localization of NS1 with hnRNPH1 was detected by fluorescence microcopy. Scale bars represent 25 and 10 μm. (E) PR8 (MOI = 0.1) infected A549 cells were lysated at 4, 6, 8 h.p.i. Nucleus and cytopastic mRNA were separated, and the mRNA level of hnRNPH1 and NS1 was detected using qPCR. The relative amounts of Nucleus/cytoplasm mRNA were determined using the comparative ($2^{-\Delta\Delta Ct}$) method. Values are means ± S.D. (n = 3). *$p < 0.05$, **$p < 0.01$, ***$p < 0.001$ vs. Mock.

hnRNPH1. Furthermore, hnRNPH1 overexpression significantly increased the levels of IFN-β mRNA and hnRNPH1 knockdown significantly reduced the levels of IFN-β, Mx1 and ISG15 mRNAs (Figure S4A and 4B). Interestingly, in the absence of virus, hnRNPH1 itself was able to significantly reduce the levels of several interferon factors (Figure S4C), which may be related to the splicing function of hnRNPH1 itself on mRNAs. In addition, in the interferon-deficient Vero cells, both hnRNPH1 overexpression and knockdown had nearly no significant effect on the expression of virus mRNAs and proteins (Figure S4D-G), suggesting that the regulation of virus replication by hnRNPH1 is indeed interferon-related manner.

Moreover, NS1 and hnRNPH1 both were reported to be associated with cell apoptosis, so we next investigated the influence of their interaction on the apoptotic pathway. The changes of apoptosis-related signalling molecules at different time points after IAV infection were first determined using western blot (Figure 5(F)). The results showed that the activation levels of PI3 K, Akt, and Bcl-2, the key components of anti-apoptosis pathway, exhibited an initial increase followed by a decrease, which may be due to the influence of NS1 on host anti-apoptosis signalling. Meanwhile, the pro-apoptotic signal protein Bax exhibited a continuous decrease within 5 h before increase in the later stages of infection. The upstream pro-apoptotic protein p-p53 initially increased within 2 h and then decreased due to the effects of PI3 K and Akt signals, but reached to the peak at 7 h.p.i. (Figure S4H and Figure 5C). Thus, the timepoint of 7 h.p.i. was selected for subsequent experiments.

Subsequently, the influence of hnRNPH1 overexpression on apoptosis was evaluated by western blotting at 7 h.p.i.. The overexpression of hnRNPH1 (4 μg) significantly increased the activation levels of anti-apoptosis protein such as PI3 K and Bcl-2, and decreased the levels of p-p53 in A549 cells (Figure S4I and Figure 5(G)), suggesting hnRNPH1 overexpression possesses the negative regulation on apoptotic pathway. Conversely, hnRNPH1 interference (80, 120 nM) led to a notable increase in the levels of p-p53 in A549 cells (Figure S4J and Figure 5(H)). These findings suggest that hnRNPH1 may have a crucial role in cell cycle regulation under viral infection conditions. Since the most significant alterations were observed in p53 level due to changes in hnRNPH1 levels, the interaction between hnRNPH1-

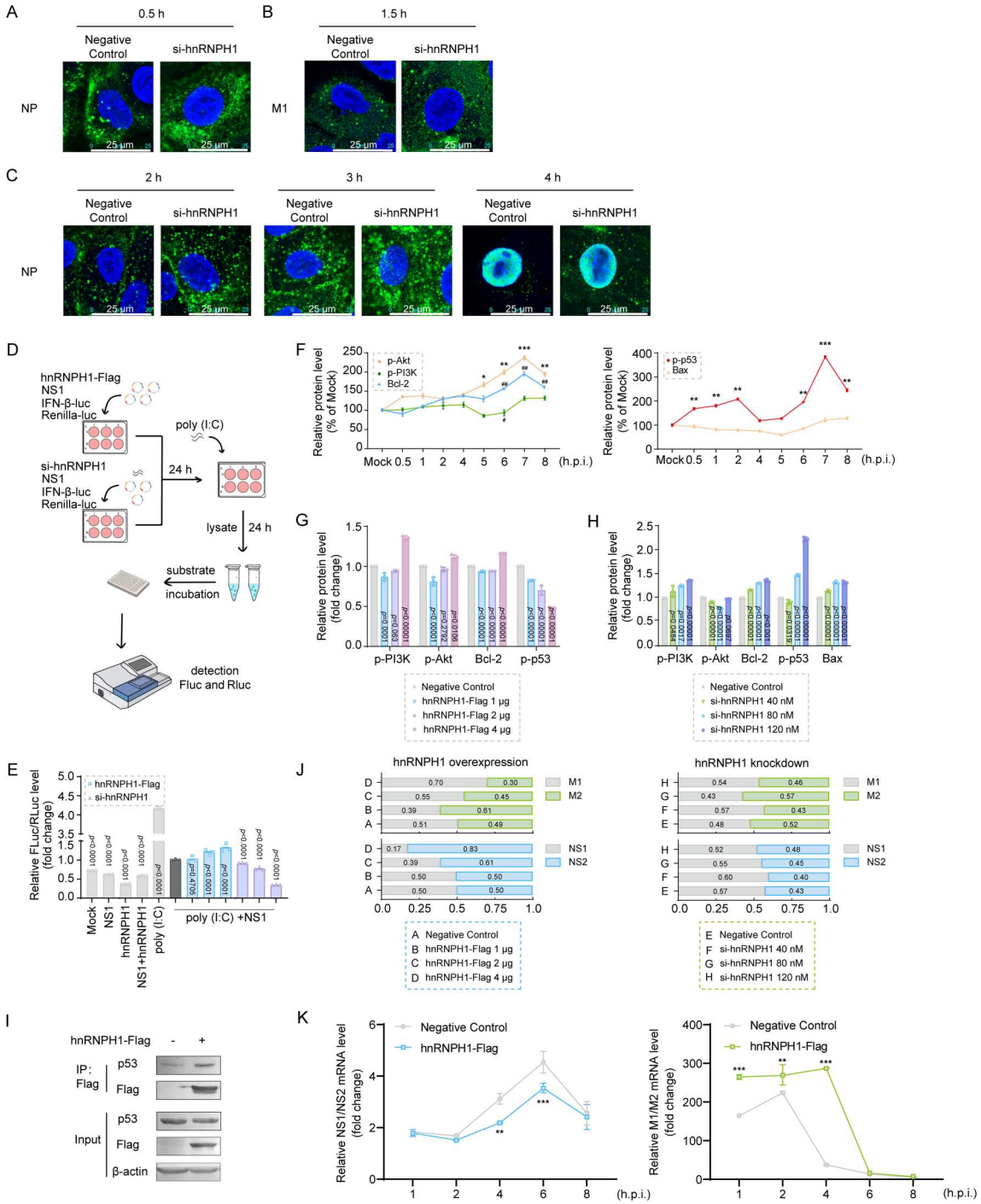

Figure 5. hnRNPH1 affects NS1 function by regulating IFN-β, apoptosis and NS1 splicing. (A-C) PR8 (MOI = 10) infected A549 cells were were fixed at 0.5 h.p.i. (A), 1.5 h.p.i. (B), and 2–4 h.p.i. (C), then the virus NP protein or M1 protein were detected by fluorescence microcopy. Scale bars represent 25 μm. (D) The flowchart of NS1 interferon inhibition assay. 293 T cells were transfected with NS1, IFN-β-Luc and hnRNPH1-Flag or si-hnRNPH1. Poly (I:C) was transfected after 16 h. And the expression of luciferase was examined after 16 h. (E) All groups were transfected with IFN-β-Luc and plasmids labelled on the figure. Values are means ± S.D. (n = 3). *P* values vs. (IFN-β-Luc + poly (I:C) + NS1) are shown in the figure. (F) Different proteins of the apoptotic pathway after PR8 infection (MOI = 0.1) were detected at different moments. The protein level was revealed by western blot. The relative amounts of proteins were determined using Image J as fold change after normalized to tubulin. Values are means ± S.D. ($n = 3$). *$p < 0.05$, **$p < 0.01$, ***$p < 0.001$, #$p < 0.05$, ##$p < 0.01$ vs. Negative Control. (G and H) The effects on apoptosis after overexpression or interference of hnRNPH1 were investigated. A549 cells were transfected with hnRNPH1-Flag (G) or si-hnRNPH1 (H). At 36 h post-transfection, cells were infected with PR8 (MOI = 0.1). The protein level was revealed by western blot. The expression level was quantified using Image J as fold change after normalized to tubulin. Values are means ± S.D. ($n = 3$). *P* values vs. Negative Control are shown in the figure. (I) 293 T cells were transfected with hnRNPH1-Flag and lysates were collected 24 h after overexpression. Lysates were incubated with anti-Flag magnetic beads overnight. Then endogenous p53 protein was detected using western blot. (J and K) A549 cells were transfected with hnRNPH1-Flag or si-hnRNPH1. At 36 h post-transfection, cells were infected with PR8 (MOI = 0.1). The RNA levels of NS1, NS2, M1 and M2 at different time were detected by qPCR. The relative amounts of NS1/NS2 and M1/M2 mRNAs were determined using the comparative ($2^{-\Delta\Delta Ct}$) method. Values are means ± S.D. (n = 3). *P* values vs. Negative Control are shown in the figure.

Flag and endogenous p53 was detected in 293 T cells (Figure 5(I)). hnRNPH1 can interact with endogenous p53, which indicated that hnRNPH1 may potentially interact with p53, thereby influencing the regulatory impact of NS1 on apoptosis.

Then, since hnRNPH1 appears mainly as a splicing factor in the present study, we further evaluated the impact of hnRNPH1 on RNA splicing of NS1 and M1 by using qRT-PCR (Figure 5(J)). Notably, hnRNPH1 overexpression led to a marked increase in the RNA levels of NS2, whereas our previous findings indicated that it suppressed NS1 RNA levels (Figure 2(E)). These results suggest that hnRNPH1 may facilitate the splicing of NS1 to NS2, thereby impeding NS1's promotion of viral protein translation.

Meanwhile, the RNA level of M2 was gradually reduced after hnRNPH1 overexpression, suggesting that hnRNPH1 affects its promotion of M1 splicing through inhibition of NS1 [22], which plays an important role in the outgrowth release of influenza virus and membrane fusion (Figure 5(J)). Conversely, hnRNPH1 knockdown slightly increased the RNA level of NS2 and M1 splicing, suggesting that the absence of hnRNPH1 has mild impact on splicing because of the presence of other host splicing factors. We also evaluated the influence of hnRNPH1 overexpression on virus NS1 and M1 mRNA splicing at different time points after viral infection by using qPCR. The results indicated that hnRNPH1 overexpression decreased the ratio of NS1/NS2 at late stage (4 and 6 h p.i.), and increased the ratio of M1/M2 at early stage (from 1 to 4 h p.i.) (Figure 5(K)), suggesting that hnRNPH1 may regulate different viral mRNA splicing at different stages.

GYR-NLS domain of hnRNPH1 interact with the RBD domain of NS1

Since hnRNPH1 can interact with NS1 to regulate its function, we were curious about which region of hnRNPH1 contributes to its binding to NS1. For this purpose, we first constructed different fragments VN173-hnRNPH1-ΔGY, VN173-hnRNPH1-ΔR3GY, and VN173-hnRNPH1-R1R2 (Figure 6(A)). The results of confocal imaging showed that none of the single-transfected groups exhibited fluorescence, but strong fluorescence could be observed in the positive control group, eliminating the possibility of self-luminescence (Figure 6(B)). However, contrary to our expectation, all of the co-transfected groups have fluorescence despite differences in intensity. Interestingly, the ΔGY and ΔR3GY fragments displayed fluorescence only in the nucleus, whereas the R1R2 mutant exhibited the fluorescence mainly in the cytoplasm (Figure 6B). This result indicates that hnRNPH1, upon deletion of its nuclear localization signal (NLS), lost its ability to enter the nucleus. Furthermore, the BiFC experiment illustrates that the binding regions of hnRNPH1 and NS1 may occupy the majority of gene fragments, and the deletion of specific gene segments does not completely disrupt their interaction. Thus, further investigation is warranted to determine the precise interaction sites between hnRNPH1 and NS1.

To further investigate the interaction sites of hnRNPH1 and NS1, molecular docking was performed. Since NS1 exists mainly as a "Y" dimer in cells, the interaction between NS1 dimer and hnRNPH1 full-length was first simulated using AlphaFold3 (Figure 6(C)). Based on the analysis of the docking result, the binding sites of NS1 are all in its RBD domain, while the binding sites of hnRNPH1 are distributed in its RRM (RRM1, 10–92 aa; RRM2, 111–190 aa; RRM3, 288–366 aa) domains (Table S3). Afterwards, we also docked H3N2-NS1 (FigureS5A and Table S5) or WSN-NS1 (Figure S5B and Table S6) with hnRNPH1 and found that the docking sites of H3N2-NS1 was similar to those of PR8-NS1, distributed in its RBD region. However, the docking results of WSN-NS1 were different from those of PR8 in that the docking sites were mainly distributed in its ED region, which may account for the weaker effect of hnRNPH1 on WSN infection. Homologous sequence analyses of the three showed that the sequences of H3N2-NS1 and PR8-NS1 near the docking sites were identical (Figure S5C).

Meanwhile, we co-transfected NS1-Flag and different truncated mutants of hnRNPH1 into 293 T cell to explore the binding regions between NS1 and hnRNPH1. The results of co-IP assay indicated that hnRNPH1 lost its interactions with NS1 after deletion of the GYR-NLS region (Figure 6(D)). After that, we produced different point mutants of NS1 and hnRNPH1 according to the molecular docking results, and further explored the binding sites using co-IP assay. The results showed that the NS1-D34A, R37A, S48A (Figure 6(E)) and hnRNPH1-F268A, T286A (Figure 6(F)) mutations influenced the binding of NS1 to hnRNPH1. In addition, we also explored the effects of hnRNPH1 point mutations on viral infection in PR8 virus infected A549 cells. The results indicated that the inhibitory effect of hnRNPH1 over-expression on virus multiplication sharply weakened after the mutation of F268 and T286 of hnRNPH1 (Figure 6(G)).

In summary, the results of molecular docking revealed that NS1 primarily interacts with hnRNPH1 through its RBD domain. In contrast, hnRNPH1 interacts with NS1 mainly through its RRM domain, which is consistent with the previous BiFC findings. Notably, the NLS in GYR plays a crucial role in regulating the nuclear translocation of hnRNPH1.

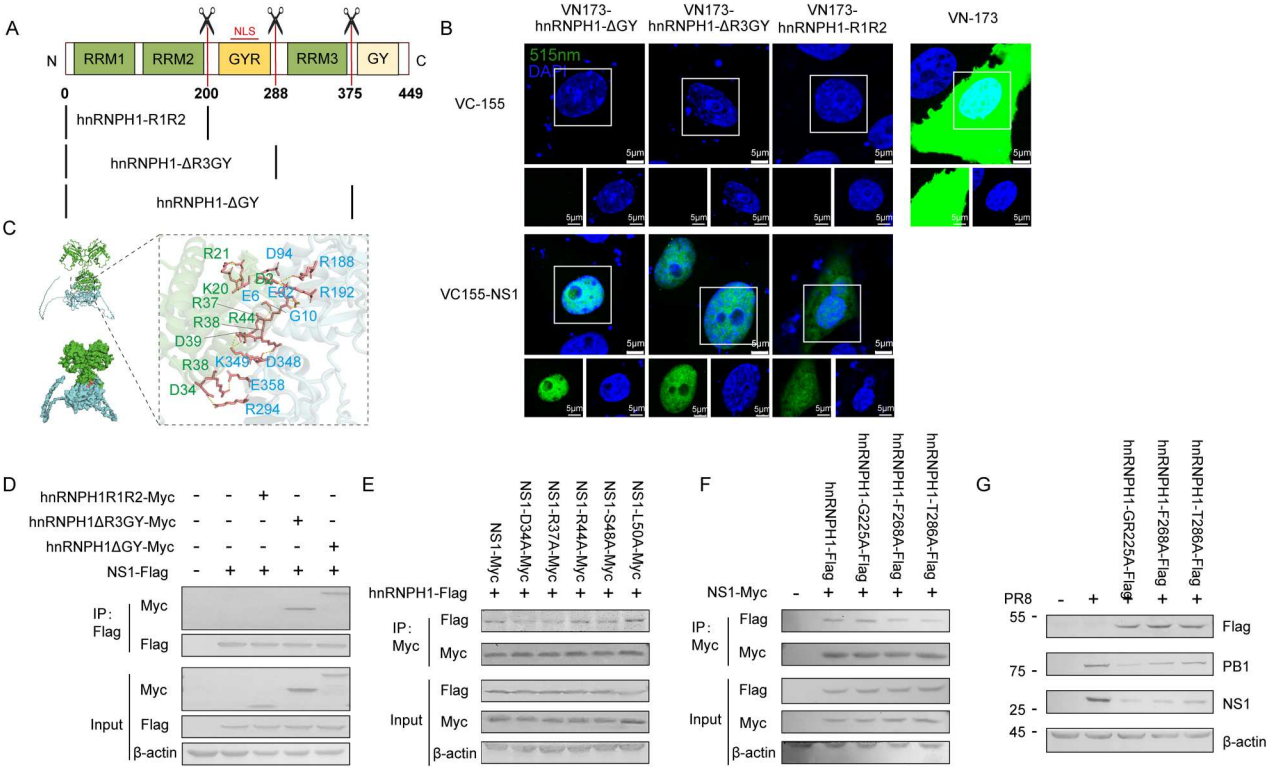

Figure 6. GYR-NLS domain of hnRNPH1 interact with the RBD domain of NS1. (A) Three different fragments of hnRNPH1. (B) A549 cells were transfected with VC155-NS1 and VN173-hnRNPH1-ΔGY, ΔR3GY, R1R2. At 36 h post-transfection, cells were fixed and the co-localization of NS1 with hnRNPH1 was detected by fluorescence microcopy. Scale bar represents 5 μm. (C) The molecular docking results for PR8-NS1 and hnRNPH1. Docking sites of NS1 dimer with hnRNPH1 full length are shown in the figure. (D) Different hnRNPH1 fragments and NS1 interaction sites were validated of by Co-IP. NS1 and hnRNPH1 fragments were co-transfected into 293 T. Then the hnRNPH1-Flag was fished using anti-Myc magnetic beads binding NS1-Myc. (E and F) Validation of the interaction sites between NS1 and hnRNPH1 using Co-IP assay with the different point mutant plasmids of NS1-Myc (E) and hnRNPH1-Flag (F), respectively. (G) A549 cells were transfected with plasmids expressing different point mutants of hnRNPH1. At 36 h post-transfection, cells were infected with PR8 (MOI = 0.1). Then the protein levels of hnRNPH1, virus PB1 and NS1 was detected by western blot.

Discussion

In recent years, there has been numerous studies on the interactions between influenza viruses and host proteins, with a particular focus on NS1 as a crucial virulence factor in influenza viruses. Through conducting experiments to identify NS1-interacting proteins and initial mechanistic investigations, we have discovered that the host protein hnRNPH1 played a role in nuclear export and post-transcriptional processing of IAV, and it interacted with NS1 to regulate IAV replication. Our study has led to the formulation of a reasonable mechanism of action for the two interacting proteins (Figure 7). Upon entry into cells, IAV triggers changes in interferon and apoptosis signalling pathways. NS1, in this context, inhibits interferon production and modulates apoptosis. hnRNPH1, by acting as a transcriptional splicing factor, facilitates NS1 splicing and modifies the apoptotic pathway, curtailing NS1's capacity to enhance viral replication (Figure 7). Thus, hnRNPH1 is a multifunctional NS1-binding protein which can regulate IAV infection via interference of the functions of NS1.

The hnRNPs mostly localize in the nucleus during steady state and shuttle from the nucleus to the cytoplasm in response to various cellular stress conditions such as HEV infection [23, 24]. In IAV infected cells, hnRNPH1 mainly binds to NS1 in the cell nucleus and the interaction between NS1 and hnRNPH1 was confirmed further by using a pull-down assay and Co-IP. Notably, the co-localization studies revealed that hnRNPH1 initially co-localized with NS1 in the nucleus, but the cytoplasmic co-localization increased with prolonged infection time. Moreover, hnRNPH1 overexpression possesses a negative regulation effect on influenza virus infection. NS1 is capable of facilitating the release of progeny virus during late stages of infection through its interaction with p53 to induce apoptosis [25], while hnRNPH1 has also been implicated in apoptotic processes [26,27]. Our study demonstrated that, interference with hnRNPH1 stimulated apoptosis, and facilitated virus release. So the expression of hnRNPH1 increased at early stage and decreased after 4 h post-infection may be related to the inhibition of NS1. Furthermore, our investigation into the splicing function of hnRNPH1 revealed

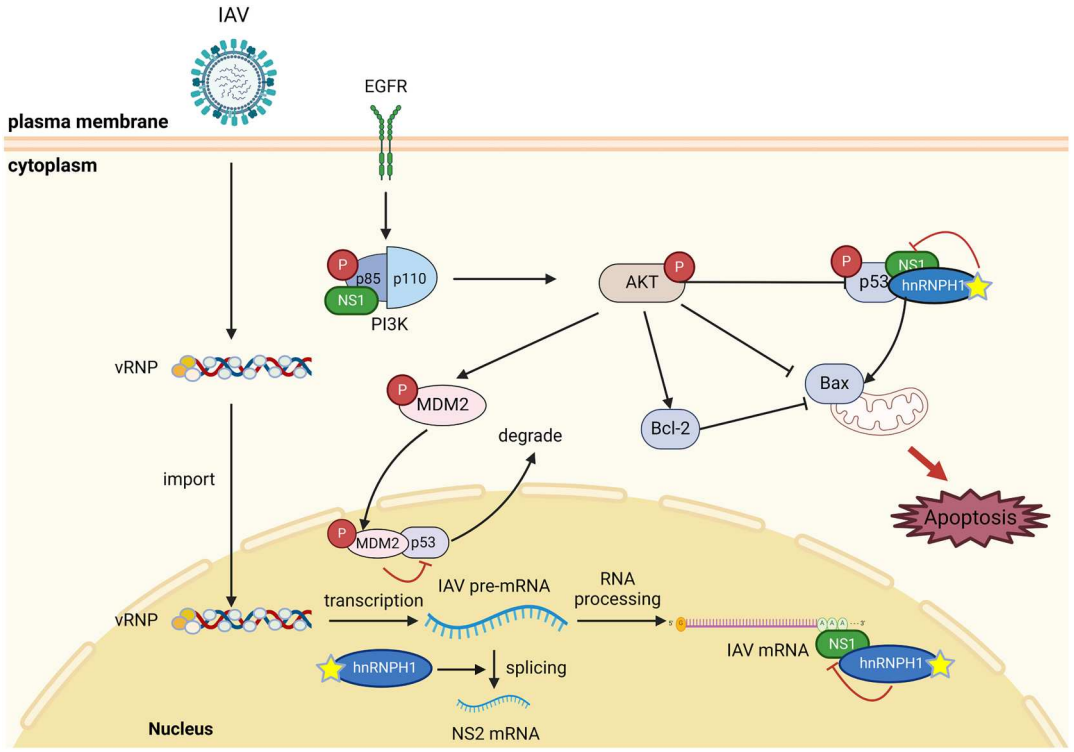

Figure 7. Hypothetical mechanistic map about the effects of hnRNPH1 on IAV proliferation. The yellow stars are hnRNPH1, a newly identified NS1-interacting protein. After apoptotic signalling is picked up by EGFR receptor on cell membrane, the signal is then transmitted to the PI3 K/Akt pathway, followed by activation of downstream Bcl-2 and MDM2 expression, which activates apoptosis and inhibits downstream Bax and p53, as well as activating the degradation of p53 by MDM2. hnRNPH1 may be able to affect viral proliferation by regulating p53 levels and also capable of disrupting the transcriptional replication of IAV by affecting the splicing of NS1 to NS2, thereby affecting viral proliferation.

that hnRNPH1 significantly enhanced the splicing of NS1 to NS2, thereby impeding the functionality of NS1. Simultaneously, hnRNPH1 exerts a certain inhibitory effect on M1 splicing, potentially hindering the release of progeny virus by suppressing the production of M2. Therefore, hnRNPH1 can regulate different viral mRNA splicing at different stages to regulate the vRNP export and virus release of IAV.

Elucidating the interaction sites of hnRNPH1 and NS1 is important for revealing the regulation roles of hnRNPH1 in IAV replication. Molecular docking indicates that NS1 dimer exhibits good interaction with hnRNPH1 and forms multiple hydrogen bonds with one another. NS1 primarily interacts with hnRNPH1 through its RBD structural domain. In contrast, hnRNPH1 may interact with NS1 mainly through the RRM domains. Notably, the NLS in GYR plays a crucial role in influencing regulating the nuclear translocation of hnRNPH1, while the RRM2 region may impacts the binding affinity of hnRNPH1 to RNA. Therefore, the RBD domain of NS1 and the RRM and NLS regions of hnRNPH1 are major regions for their interaction. In addition, the D34, R37, S48 of NS1 and F268, T286 of hnRNPH1 may be required for the binding of NS1 to hnRNPH1. The protein crystallization analysis will be needed to further verify the specific interaction sites between NS1 and hnRNPH1 in the future.

NS1 is reported to antagonize the natural immune response of the host and the RBD region of NS1 play an important role in its binding to dsRNA and the antagonism of interferon. In this study, we found that overexpression of hnRNPH1 can restore the production of IFN-β which was reduced by NS1 and hnRNPH1 knockdown significantly reduced the expression of IFN-β, Mx1 and ISG15 mRNAs, suggesting that the upregulation of interferon by hnRNPH1 may be due to its binding to the RBD region of NS1. Among the NS1-interacting proteins identified so far, CPSF30 is able to bind to the ED region of NS1 and promote the inhibition of host gene expression by NS1 [28]. Binding of PABP1 and eIF4G1 to the NS1-RBD region promotes the recruitment of viral mRNA [29]. PABP2 is reported to be able to bind to the NS1-ED region which can promote the inhibition of the maturation of host mRNAs by NS1 [30]. NXF1 binding to NS1 can promote the nuclear export of viral mRNAs but the inhibition of host mRNA export [31]. However, hnRNPH1, as a splicing factor and RNA-binding protein, can bind to the RBD region of NS1 to inhibit the multi-function of NS1 so as to reduce virus infection, rather than being hijacked by NS1 to promote viral replication, which is a distinguishing feature of hnRNPH1 from other proteins.

Conclusion

In conclusion, this study proved for the first time that the cellular protein hnRNP H1 could interact with IAV NS1 protein to influence IAV replication. A crucial aspect of our findings is that hnRNP H1 functions as a transcriptional splicing factor, facilitates NS1 splicing and modifies the apoptotic pathway, curtailing NS1's capacity to enhance viral replication. However, NS1 can in turn antagonize the expression and function of hnRNPH1. Thus, regulation of the interaction between hnRNP H1 and NS1 protein may be an alternative strategy for the control of IAV infection.

Disclosure statement

No potential conflict of interest was reported by the author(s).

Funding

This work was supported by National Natural Science Foundation of China (82173860); Natural Science Foundation of Shandong Province (ZR2019ZD18). Natural Science Foundation of Shandong Province.

Credit author statement

Jinyu Wang: Writing-Original Draft, Data curation, Formal analysis, Investigation. **Yang Zhang:** Validation, Formal analysis, Investigation. **Lishan Sun:** Methodology, Validation. **Zihan Wang:** Data curation. **Cui Hao:** Conceptualization, Supervision, Writing-Reviewing and Editing. **Wei Wang:** Conceptualization, Supervision, Writing-Reviewing and Editing, Funding acquisition.

ORCID

Wei Wang http://orcid.org/0000-0002-6548-6422

References

[1] Gaitonde DY, Moore FC, Morgan MK. Influenza: diagnosis and treatment. Am Fam Physician. 2019;100:751–758.
[2] Krammer F, Smith GJD, Fouchier RAM, et al. Influenza. Nat Rev Dis Primers. 2018;4:3. doi:10.1038/s41572-018-0002-y
[3] Mcgeoch D, Fellner P, Newton C. Influenza virus genome consists of eight distinct RNA species. P Natl Acad Sci USA. 1976;73:3045–3049. doi:10.1073/pnas.73.9.3045
[4] Bouvier NM, Palese P. The biology of influenza viruses. Vaccine. 2008;26:D49–D53. doi:10.1016/j.vaccine.2008.07.039
[5] Eisfeld AJ, Neumann G, Kawaoka Y. At the centre: influenza a virus ribonucleoproteins. Nat Rev Microbiol. 2015;13:28–41. doi:10.1038/nrmicro3367
[6] Te Velthuis AJW, Fodor E. Influenza virus RNA polymerase: insights into the mechanisms of viral RNA synthesis. Nat Rev Microbiol. 2016;14:479–493. doi:10.1038/nrmicro.2016.87
[7] Cady SD, Luo W, Hu F, et al. Structure and function of the influenza a M2 proton channel. Biochemistry. 2009;48:7356–7364. doi:10.1021/bi9008837
[8] Calder LJ, Rosenthal PB. Cryomicroscopy provides structural snapshots of influenza virus membrane fusion. Nat Struct Mol Biol. 2016;23:853–858. doi:10.1038/nsmb.3271
[9] Brunotte L, Flies J, Bolte H, et al. The nuclear export protein of H5N1 influenza A viruses recruits Matrix 1 (M1) protein to the viral ribonucleoprotein to mediate nuclear export. J Biol Chem. 2014;289:20067–20077. doi:10.1074/jbc.M114.569178
[10] Byrd-Leotis L, Cummings RD, Steinhauer DA. The interplay between the host receptor and influenza virus hemagglutinin and neuraminidase. Int J Mol Sci. 2017;18:1541–1563. doi:10.3390/ijms18071541
[11] Vajda J, Weber D, Brekel D, et al. Size distribution analysis of influenza virus particles using size exclusion chromatography. J Chromatogr A. 2016;1465:117–125. doi:10.1016/j.chroma.2016.08.056
[12] Rosário-Ferreira N, Preto AJ, Melo R, et al. The central role of non-structural protein 1 (NS1) in influenza biology and infection. Int J Mol Sci. 2020;21:1511–1535. doi:10.3390/ijms21041511
[13] Carrillo B, Choi JM, Bornholdt ZA, et al. The influenza a virus protein NS1 displays structural polymorphism. J Virol. 2014;88:4113–4122. doi:10.1128/JVI.03692-13
[14] Mitra S, Kumar D, Hu L, et al. Influenza a virus protein NS1 exhibits strain-independent conformational plasticity. J Virol. 2019;93:1113–1128. doi:10.1128/JVI.00917-19
[15] Wang BX, Fish EN. Interactions between NS1 of influenza a viruses and interferon-α/β: determinants for vaccine development. J Interf Cytok Res. 2017;37:331–341. doi:10.1089/jir.2017.0032
[16] Wang W, Cui ZQ, Han H, et al. Imaging and characterizing influenza A virus mRNA transport in living cells. Nucleic Acids Res. 2008;36:4913–4928. doi:10.1093/nar/gkn475
[17] Han SP, Tang YH, Smith R. Functional diversity of the hnRNPs: past, present and perspectives. Biochem J. 2010;430:379–392. doi:10.1042/BJ20100396
[18] Gautrey H, Jackson C, Dittrich AL, et al. SRSF3 and hnRNPH1 regulate a splicing hotspot of HER2 in breast cancer cells. RNA Bio. 2015;12:1139–1151. doi:10.1080/15476286.2015.1076610
[19] Samatanga B, Dominguez C, Jelesarov I, et al. The high kinetic stability of a G-quadruplex limits hnRNP F qRRM3 binding to G-tract RNA. Nucleic Acids Res. 2013;41:2505–2516. doi:10.1093/nar/gks1289
[20] Van Dusen CM, Yee L, McNally LM, et al. A glycine-rich domain of hnRNP H/F promotes nucleocytoplasmic shuttling and nuclear import through an interaction with transportin 1. Mol Cell Biol. 2010;30:2552–2562. doi:10.1128/MCB.00230-09
[21] Tong L, Chu Z, Gao X, et al. Newcastle disease virus V protein interacts with hnRNPH1 to promote viral replication. Vet Microbiol. 2021;260:109093. doi:10.1016/j.vetmic.2021.109093
[22] Zhang K, Cagatay T, Xie D, et al. Cellular NS1-BP protein interacts with the mRNA export receptor NXF1 to mediate nuclear export of influenza virus M mRNAs. J Biol Chem. 2024;300:107871. doi:10.1016/j.jbc.2024.107871

[23] Geuens T, Bouhy D, Timmerman V. The hnRNP family: insights into their role in health and disease. Hum Genet. 2016;135:851–867. doi:10.1007/s00439-016-1683-5

[24] Pingale KD, Kanade GD, Karpe YA. Heterogeneous nuclear ribonucleoproteins participate in hepatitis E virus replication. J Mol Bio. 2020;43:2369–2387. doi:10.1016/j.jmb.2020.02.025

[25] Ampomah PB, Lim LHK. Influenza A virus-induced apoptosis and virus propagation. Apoptosis. 2020;25:1–11. doi:10.1007/s10495-019-01575-3

[26] Liu M, Yang L, Liu X, et al. HNRNPH1 is a novel regulator of cellular proliferation and disease progression in chronic myeloid leukemia. Front Oncol. 2021;11:682859. doi:10.3389/fonc.2021.682859

[27] Li Y, Bakke J, Finkelstein D, et al. HNRNPH1 is required for rhabdomyosarcoma cell growth and survival. Oncogenesis. 2018;7:9. doi:10.1038/s41389-017-0024-4

[28] Kuo RL, Krug RM. Influenza a virus polymerase is an integral component of the CPSF30-NS1A protein complex in infected cells. J Virol. 2009;8:1611–1616. doi:10.1128/JVI.01491-08

[29] Burgui I, Aragón T, Ortín J, et al. PABP1 and eIF4GI associate with influenza virus NS1 protein in viral mRNA translation initiation complexes. J Gen Virol. 2003;84:3263–3274. doi:10.1099/vir.0.19487-0

[30] Chen Z, Li Y, Krug RM. Influenza A virus NS1 protein targets poly(A)-binding protein II of the cellular 3'-end processing machinery. EMBO J. 1999;18:2273–2283. doi:10.1093/emboj/18.8.2273

[31] Zhang K, Xie Y, Muñoz-Moreno R, et al. Structural basis for influenza virus NS1 protein block of mRNA nuclear export. Nat Microbiol. 2019;4:1671–1679. doi:10.1038/s41564-019-0482-x